Determination of the Li/Nb Ratio in Lithium Niobate by Means of Birefringence and Raman Measurements

U. Schlarb, S. Klauer, M. Wesselmann, K. Betzler, M. Wöhlecke

FB Physik, Universität Osnabrück, Postfach 4469, W-4500 Osnabrück, Germany (Fax: +49-541/9692670)

Abstract. Two optical methods for the determination of the Li/Nb ratio in lithium niobate ($LiNbO_3$) are discussed. Data for the optical birefringence method are presented, they cover the entire composition range in which $LiNbO_3$ can be fabricated and a wide spectral region. The linewidths of lattice modes have been measured by means of Raman scattering as a function of the Li/Nb ratio for single crystals with polished and rough surfaces.

PACS: 78.20.Fm, 78.30.Hv, 78.30.Ly, 81.70.Dw

Because of its attractive set of electrooptical, nonlinear optical and piezoelectrical properties lithium niobate ($LiNbO_3$) is widely used for integrated optics, nonlinear optics, electrooptics, and surface acoustic wave devices. Crystals of $LiNbO_3$ can be grown in a comparably wide composition range [1, 2], Li deficits up to about 4% with respect to the stoichiometric composition are possible. As most of the physical properties are composition dependent, it is necessary to check the Li content by appropriate—preferably nondestructive—methods.

One of the earliest methods for the determination of the Li/Nb ratio makes use of the fact that the Curie temperature strongly depends on the crystal composition [3]. The method is fairly accurate yet has the drawback that the crystal under investigation has to be heated up to rather high temperatures.

Nearly all other classical techniques rely in some manner on the variation of the electronic structure, or more specific, of the dielectric tensor with the crystal composition. This variation shows up both in the real and in the imaginary part. Thus the shift of the optical absorption edge [4] or of the principal refractive indices [5] can be used for characterizing the composition of $LiNbO_3$. Most sensitive are generally techniques which use appropriate differences of the refractive indices—birefringence at a fixed wavelength, measured conventionally [6] or by holographic scattering [7, 8], or birefringence between different wavelengths, measured by nonlinear optical techniques. The latter include the measurement of the phase matching temperature [9, 10] or the phase matching angle for optical second-harmonic generation and noncollinear techniques like noncollinear frequency doubling [11].

The methods mentioned so far probe changes of the high frequency (electronic) part of the dielectric tensor with crystal composition. The ionic part is influenced as well. This is reflected in the linewidths of the lattice modes. With respect to a linewidth analysis Raman scattering is superior to infrared absorption. Therefore in the first determinations of stoichiometry variations Raman powder spectroscopy has been used [12, 13].

Here we present new birefringence data for a wide range of optical wavelengths and results on Raman linewidths for selected phonons allowing a characterization of $LiNbO_3$ samples with respect to the crystal compositions instead of melt compositions reported in most previous work. Both methods cover the whole composition range in which $LiNbO_3$ can be fabricated.

1 Principles

$LiNbO_3$ can be grown with compositions characterized by molar Li contents which range from about 46% up to 50% in the solid phase. Li deficits in nonstoichiometric $LiNbO_3$ are found to be compensated by Nb ions on Li lattice sites [14]. These additional Nb ions vary the electronic structure and thus the macroscopic dielectric tensor of $LiNbO_3$. As the compensation by Nb ions is proportional to the amount of missing Li ions, the Li deficit should show up linearly in the variations of the dielectric tensor. Such linear behaviour indeed has been found in the shift of the optical absorption edge [4, 15]. As real and imaginary part of the dielectric tensor can be referred to each other by a Kramers-Kronig analysis, one should expect a linear behaviour in the dependence of the square of the refractive indices on composition, too. As long as the variations are small, a suitable series expansion will expand the linear behaviour to the refractive indices and their difference, the birefringence.

Substitution of Li by Nb reduces the translational symmetry of the lattice, changes ionic masses and force con-

stants and may, in addition, influence the interionic potentials, in particular the degree of anharmonicity. Each of these effects contributes to the linewidths of the lattice modes. The first three affect the inhomogeneous, the last the homogeneous broadening. The reduction of translational symmetry relaxes the selection rule due to conservation of momentum. This means that the scattered phonon can assume a broad range of wavevector **k** values in the Brillouin zone. A wide distribution of the **k** vectors results in a broadening of Raman bands. Whether a symmetric or asymmetric lineshape is observed depends on the strength of the directional dispersion of the phonon modes and the ion substitution process. The Li deficit (V_{Li}) is compensated by Nb ions on Li lattice sites (Nb_{Li}) [14], as mentioned above. One unit cell with Nb_{Li} can balance four unit cells with V_{Li}. In the unit cell containing Nb_{Li} the mass increases more strongly than the mass decreases in the cells with V_{Li}. A force constant change is expected in the same manner (stronger for the first and weaker for the last), because Nb^{5+} enters a Li^+ site. The mass substitution causes an increase of the density of states at lower frequencies for Nb_{Li} units and a high frequency local mode type excitation for V_{Li} units. The strengthening of the force constant for Nb_{Li} and the weakening for V_{Li} support the effect of mass substitution. Thus the Nb_{Li} units should influence the low energy wing of the Raman bands and the V_{Li} the high energy one, presumably in different manner. Because the non-stoichiometry is governed by the Nb_{Li} concentration, in our simple model line broadening should scale linearly with Li deficiencies.

The homogeneous broadening depends on temperature, thus comparative studies have to be carried out at constant temperature.

2 Experimental

The birefringence measurements discussed here were carried out in a wavelength range from 400 to 1200 nm using several wavelengths of a tunable HeNe laser or a mercury lamp. Usually one would measure the birefringence directly for instance by a rotating sample or by a compensation method. Here we primarily measured the refractive indices using an interferometric technique where parallel plate shaped samples were rotated in one arm of a Michelson interferometer [16]. The resulting optical path length shift was measured and evaluated numerically to get the refractive indices for the respective light polarizations with an accuracy of about 5×10^{-4}. The difference between the ordinary and the extraordinary refractive index then yields the birefringence with about the same absolute accuracy.

For reasons of convenience we used conventional right-angle Raman scattering at room temperature (argon-ion laser, double monochromator, photon counting). To use Raman scattering as a standard characterization technique it is necessary to make adjustments and evaluations as simple as possible. This can be achieved when the Raman line used obeys four conditions: (1) the intensity should be high enough, (2) the line should be well separated from the laser line and should not interfere with other Raman lines, (3) the directional dispersion should be zero

or at least small, and (4) optical damage should be minimized. The fourth condition is fulfilled for laser beams travelling along the ferroelectric c- axis forcing the light polarization to be perpendicular to c. This strongly reduces photorefractive index changes which have a time dependent influence on the shape of the excited volume and thus in turn on the scattering intensity [17].

For an unambiguous determination of the linewidth Γ (full width at half maximum of the measured Raman band, irrespective of the actual lineshape) we have chosen the E and A_1 modes at 153 cm^{-1} and 876 cm^{-1}. The first three conditions are fulfilled for the high-frequency mode completely, while the 153 cm^{-1} phonon is accompanied by an additional weak band at about 175 cm^{-1} (an E_L mode [18])), which only weakly contributes to the experimental linewidth of the 153 cm^{-1} phonon. The uncertainty for Γ is 0.2 cm^{-1} for polished single crystals and 0.3 cm^{-1} for unfinished surfaces for the 876 cm^{-1} band and half of these values for the 153 cm^{-1} line.

The crystals used as calibration standards had been analyzed by an ion chromatographic method [19]. One of the crystals had been brought to the stoichiometric composition by vapour transport equilibration (VTE). The accuracy of the compositions can be assumed to be about 0.2%. The homogeneity of the crystals was checked by spatially resolved second-harmonic generation [20, 21] and found to be much better than the composition uncertainty. The typical crystal size after precise cutting and polishing was $8 \times 8 \times 8$ mm^3 well suitable for both birefringence and Raman measurements. For the calibration measurements four crystals with Li contents between 46 and 50% were used.

3 Results and Discussion

3.1 Birefringence Measurements

The typical wavelength dispersion of the optical birefringence as derived from refractive index measurements is shown in Fig. 1. Plotted are the data for $LiNbO_3$ crystals with Li contents ranging from 46.1 to 50%. The experimental values are represented by dots, the solid lines are derived from a generalized Sellmeier fit for the refractive indices [22]. The refractive indices of $LiNbO_3$ can be described by a two term Sellmeier equation of the form

$$n_i^2 = 1 + \frac{50 + c_{Li}}{100} \frac{A_{0,i}}{1 - \lambda_{0,i}^2/\lambda^2} + \frac{50 - c_{Li}}{100} \frac{A_{1,i}}{1 - \lambda_{1,i}^2/\lambda^2},$$
(1)

where A_0, A_1, λ_0, λ_1 are generalized parameters for the ordinary ($i = 0$) and the extraordinary ($i = e$) index of refraction, and $c_{Li} = mol\%$ Li_2O is the Li content of the crystal. The solid lines in Fig. 1 are the differences of the refractive indices calculated from the equation above.

In Fig. 2 the birefringence is plotted versus the Li content of the crystals. As expected, approximately linear behaviour is found. This can be described by

$$\Delta n = [c_{Li} - a(\lambda)]/b(\lambda),$$
(2)

where $a(\lambda)$ and $b(\lambda)$ are wavelength dependent parameters.

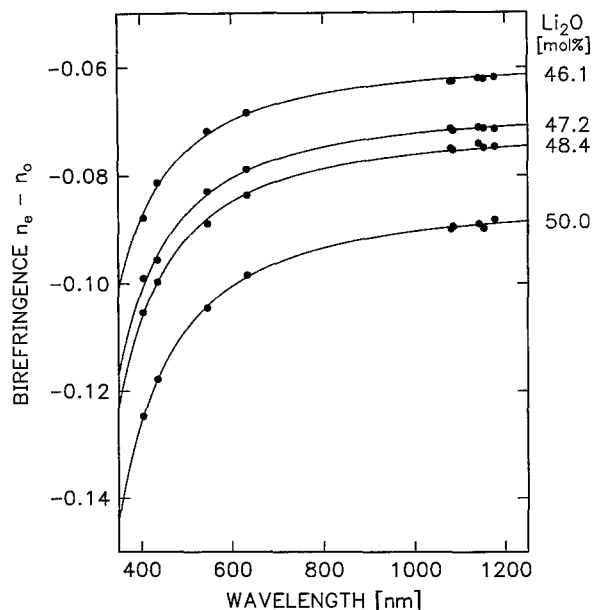Fig. 1. Dispersion of the birefringence for $LiNbO_3$ crystals with different compositions. The respective Li content is denoted
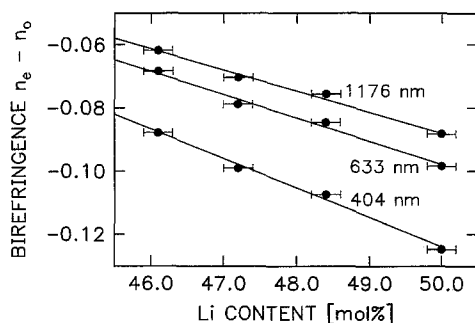

Fig. 2. Composition dependence of the optical birefringence in $LiNbO_3$ for different optical wavelengths

Transposing the equation to

$$c_{Li} = a(\lambda) + b(\lambda)\Delta n \qquad (3)$$

makes it suitable for characterizing the crystal stoichiometry by birefringence measurements.

The birefringence parameters a and b can be derived from the discussed generalized Sellmeier equation. The calculated values are shown in Fig. 3 together with the experimental values for various wavelengths. Numerical values for several wavelengths of the mercury lamp and the HeNe laser are given in Table 1.

The wavelength dependence of the birefringence parameters shows that the birefringence method for crystal characterization is slightly more sensitive when applied in the short wavelength region.

3.2 Raman Masurements

The shapes of the E-phonon at 153 cm^{-1} and the mode at 876 cm^{-1} with predominant A_1 character are shown in Fig. 4. The 153 cm^{-1} band has been measured in the Z(YZ)X
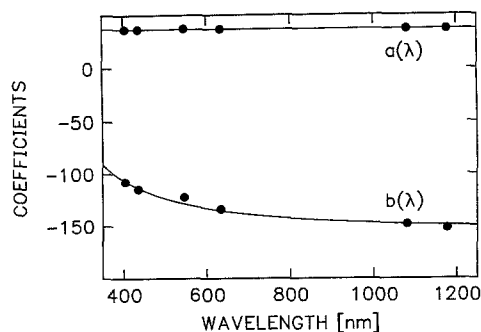

Fig. 3. Wavelength dependence of the birefringence parameters a and b (see text) for $LiNbO_3$. Calculated values are given by solid lines, experimental values (linear least-squares fits to the measured birefringence data) by dots

Table 1. Parameters $a(\lambda)$ and $b(\lambda)$ of (3) for several wavelengths

λ [nm]	$a(\lambda)$	$b(\lambda)$
404.66	36.72	−107.20
435.83	36.68	−113.83
546.07	36.70	−128.79
633.00	36.73	−135.46
1079.81	36.85	−148.12
1176.68	36.86	−149.17

and the 876 cm^{-1} in the Z(YY)X configuration. For both bands the linewidth is continuously increasing with decreasing Li content. On the other hand the frequency of the bandmaxima varies less than 0.2 cm^{-1} over the whole composition range. This minor dependence is not sufficient for an easy and accurate compositional check. The low-frequency E-mode shows an almost symmetrical broadening, while the high-frequency mode clearly becomes asymmetric. No influence of the scattering volume on the bandwidth has been observed for undoped crystals because of the high transparency in the visible. Raman spectra of samples grown from congruent melts in different crystal growth laboratories coincide with respect to the bandshape within experimental uncertainties. Most critical is the determination of the baseline. Therefore we extended the measured spectral range for each band as much as possible. This uncertainty in the determination of the baseline governs the accuracy of the method and eliminates the use of other phonon modes.

In order to separate the homogeneous and inhomogeneous contributions to the linewidths we investigated the temperature dependence of Γ. For both modes Γ decreases continuously down to T $\approx$ 70 K. For lower temperatures Γ is constant, exhibiting the inhomogeneous contribution. Apart from additive constants, the temperature dependences $\Gamma(T)$ are equal for all crystals investigated. This equality suggests that the anharmonicity of the interionic potentials are only weakly influenced by the increase in disorder.

The halfwidths Γ of both bands determined at room temperature are plotted versus crystal composition in Fig. 5. The dependence is approximated by a linear least-squares fit yielding
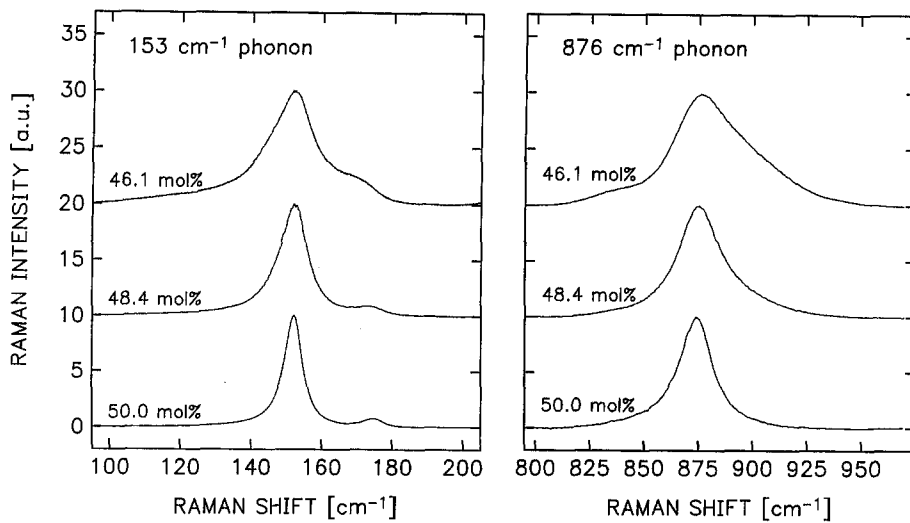
Fig. 4. Shapes of the 153 cm^{-1} and the 876 cm^{-1} Raman lines in LiNbO$_3$ for different crystal compositions
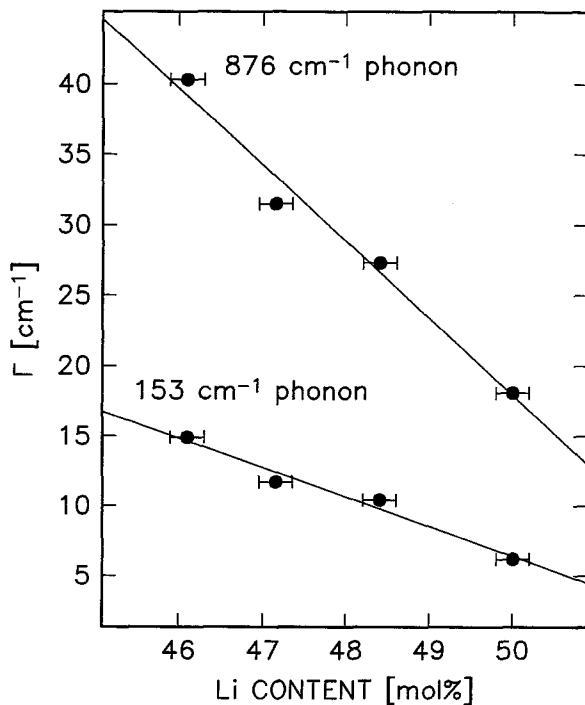

Fig. 5. Halfwidths of the Raman lines at 153 cm^{-1} and 876 cm^{-1} in LiNbO$_3$ vs Li content. The dots are the experimental values, the lines represent the least-squares fits

$$c_{Li}[\text{mol}\%] = 53.03 - 0.4739 \, \Gamma[\text{cm}^{-1}] \qquad (4)$$

for the 153 cm^{-1} phonon and

$$c_{Li}[\text{mol}\%] = 53.29 - 0.1837 \, \Gamma[\text{cm}^{-1}] \qquad (5)$$

for the 876 cm^{-1} band.

If no polished single crystals are at hand, the Raman technique works for boules with one properly aligned unfinished surface. In this case the exciting laser beam should hit the surface under grazing incidence. Due to the tedious stray light in this scattering geometry baseline problems are enhanced. Therefore we suggest to use the 876 cm^{-1} mode only. We have found that (5) still applies when the constant is changed to 54.8.

3.3 Accuracy

To check and to compare the accuracies of the described characterization methods the Li contents of two LiNbO$_3$ crystals with up to then unknown compositions were determined. Birefringence measurements at three different wavelengths (404, 633 and 1176 nm) and Raman scattering of the two Raman modes (153 and 876 cm^{-1}) have been performed. All measurements resulted in nearly identical concentration values for both test crystals (48.6 and 49.2 mol% Li, respectively). Two aspects of this result will be discussed in more detail. First, we consider the relative accuracy of each method when applied to a set of samples. According to (3) the experimental uncertainty of the birefringence data (5×10^{-4}) corresponds to a resolution of the Li content of 0.05 mol% Li$_2$O. The estimated uncertainties in the Raman linewidths of 0.2 cm^{-1} for the 876 cm^{-1} and 0.1 cm^{-1} for the 153 cm^{-1} band yield again a compositional resolution of 0.0.5 mol% Li$_2$O. Thus with both methods the same resolution for c_{Li} can be achieved. Second, the concentrations determined with both methods coincide within the resolution limits given above. The calibrations for both methods are consistent. This justifies the assumption that series expansions up to the term linear in concentration for each of the respective physical properties are appropriate.

However, the absolute accuracies of both methods depend on the exactness of the concentration data for the standard crystals used. The uncertainties of the concentration data of 0.2 mol% govern the absolute accuracies of the described methods.

4 Conclusion

The data presented show that both the optical birefringence and the Raman scattering method are techniques well suitable for a simple, nondestructive determination of the Li/Nb ratio in lithium niobate crystals. Each of the methods exhibits excellent accuracy, both relative and absolute. No restrictions have been found for the concentration range of LiNbO$_3$ in which the techniques are applicable. Both are room-temperature methods, thus no heat-

ing or cooling of the samples is necessary. Moreover, Raman scattering is suitable also for nonideal samples.

References

1. L.O. Svaasand, ·M. Erikstrud, G. Nakken, A.P. Grande: J. Crystal Growth **78**, 230 (1974)
2. A. Räuber: Current Topics in Material Science **1** (North Holland, Amsterdam 1978) p. 481
3. J.R. Carruthers, G.E. Peterson, M. Grasso, P.M. Bridenbaugh: J. Appl. Phys. **42**, 1846 (1971)
4. I. Földváry, K. Polgár, R. Voszka, R.N. Balasanyan: Crystal Res. Technol. **19**, 1659 (1984)
5. J.G. Bergman, A. Ashkin, A.A. Ballman, J.M. Dziedzik, H.J. Levinstein, R.G. Smith: Appl. Phys. Letters **12**, 92 (1968)
6. E. Born, E. Willibald, R. Veith: Proc. IEEE Ultrasonics Symp. **1**, 268 (1984)
7. L. Arizmendi: J. Appl. Phys. **64**, 4654 (1988)
8. U. van Olfen, R.A. Rupp, E. Krätzig, B.C. Grabmaier: Ferroelectrics Letters **10**, 133 (1989)
9. N. Schmidt, K. Betzler, B.C. Grabmaier: Appl. Phys. Letters **58**, 34 (1991)
10. P.F. Bordui, R.G. Norwood, D.H. Jundt, M.M. Fejer: J. Appl. Phys. **71**, 875 (1992)
11. A. Reichert, K. Betzler: Ferroelectrics **126**, 9 (1992)
12. B.A. Scott, G. Burns: J. Am. Ceram. Soc. **55**, 225 (1972)
13. A.E. Balanevskaya, L.I. Pyatigorskaya, Z.I. Shapiro, L.N. Margolin, E.A. Bovina: J. Appl. Spectrosc.-(Engl. Transl.) **38**, 491 (1983)
14. S.C. Abrahams, P. Marsh: Acta Cryst. **B42**, 61 (1986)
15. N. Schmidt: Ph. D. Thesis, Universität Osnabrück (1989)
16. U. Schlarb, K. Betzler: Ferroelectrics **126**, 39 (1992)
17. M. Nippus, R. Claus: Z. Naturforsch. **33a**, 924 (1978)
18. X. Yang, G. Lan, B. Li, H. Wang: Phys. Status Solidi (b) **141**, 287 (1987)
19. B.C. Grabmaier, F. Otto: J. Crystal Growth **79**, 682 (1986)
20. N. Schmidt, K. Betzler, S. Kapphan: Cryst. Latt. Def. and Amorph. Mat. **15**, 103 (1987)
21. N. Schmidt, K. Betzler, M. Grabs, S. Kapphan, F. Klose: J. Appl. Phys. **65**, 1523 (1989)
22. U. Schlarb, K. Betzler: unpublished